EXPERIMENTAL CHARACTERISATION OF RECYCLED (GLASS/TPU WOVEN FABRIC) FLAKE REINFORCED THERMOPLASTIC COMPOSITES

M.I. Abdul Rasheed*, B. Rietman, H.A. Visser, R. Akkerman
Faculty of Engineering Technology, University of Twente, Enschede, The Netherlands
*Corresponding author (m.i.abdulrasheed@utwente.nl)

Keywords: *Discontinuous random flake, thermoplastic composites, experimental analysis*

1 Abstract

Recycling of continuously reinforced thermoplastic composites (TPC) has a substantial prospect at present and in future due to its increasing availability and rapidly growing application regime. This study focusses on the first steps in using TPC process scrap on a scale in which its maximum potential can be utilised. It entails the mechanical response viz. elastic properties and strength of the flake reinforced plates under uniaxial tension. The plates were manufactured by compression moulding of flakes made of woven glass fabric reinforced thermoplastic polyurethane (TPU), oriented randomly within the plate. The randomness in the orientation of the flakes is evident from the observed in-plane isotropic behaviour in the experiments. Failure is in most cases dominated by the matrix and changes its path to avoid the flakes. The failure surface observation revealed regions of good and also regions of poor fibre-matrix as well as flake-matrix adhesion. Different classes of flake sizes were used to produce plate samples. The relationship between the flake size and mechanical properties were not statistically significant due to the similarities observed in the size distribution between the different classes of flakes used. The measured strength and stiffness values are compared with existing values and analytical results. The analytical results for stiffness and strength were found to be close to the measurements by 8% on average, which shows a fairly good agreement of the idealised theory where the effect of interactions between reinforcements are not included.

2 Introduction

The rising demand in reducing the throughput time of components produced from composite materials leads to an increase in application of thermoplastic composites. The inherent property of thermoplastics of being able to be recycled makes it a more viable choice in an economical and ecological point of view than thermosets.

The increase in the production of TPC implicitly poses a problem of process scrap management [1]. The high potential in the TPC scrap can be exploited by downgrading them one level into recycled products, which has promising applications in industrial and consumer products. Combined with the features of high performance thermoplastics, like high fracture toughness and environmental stability, it can offer a wide range of properties and also enable various joining abilities.

The concept of using discontinuous reinforcements has been in existence for the past few decades [10-17]. Different forms of materials are available viz. bulk moulding compounds (BMC) with short fibre reinforcements (up to 12 mm) in the form of a dough, sheet moulding compounds (SMC), a sheet like preform with long fibres (up to 50 mm) oriented randomly. Processes like injection moulding and compression moulding are used to manufacture products from these material forms. These processes induce flow and hence reorient the reinforcements depending on the process used. In a view to improve the properties of SMC, chopped fibres are replaced with chopped tapes/prepregs (HexMC®) by Hexcel [2]. Similar form of chopped unidirectional prepregs in bulk form is also used for one-shot three dimensional moulding [3] from TenCate. These materials have virgin raw materials and are used in automotive and recently in aerospace applications. The typical aerospace applications include high volume products such as clips, brackets and parts such as window frames [4,5]. On the other hand this article investigates the usage of TPC recyclates in bulk form.

In this study the recycling is limited to grinding the composite scrap into flakes of smaller dimensions, in order to conserve the parent materials' properties such as the reinforcing effect of fibres in a weave pattern as much as possible. The ground flakes can be moulded directly into flake-reinforced composite (F-RC) parts without the addition of extra neat resin.

The molded flake-reinforced composite has a matrix phase contributed by the matrix material present in the flakes and a reinforcement phase contributed by the reinforcements in the flakes, in an ideal condition. The F-RC plates used in this study contain loose fibre particles which is a byproduct of the grinding process as shown in Figure 13.

Unlike short fibres [6], irrespective of the preferential orientation, the flakes provide a two-dimensional reinforcement and hence enhanced quasi-isotropic in-plane properties. The end products' properties are a function of the statistical size distribution and orientation distribution of the flakes analogous to the short fibre reinforced composites (SFRC) [7,8]. However, in F-RC it is also essentially a function of various other parameters like overlap between flakes [9], agglomeration and interface properties in addition to voids and matrix micro-cracks in the matrix phase.

Several theories for determining the theoretical modulus and strength of discontinuous reinforced composites have been developed and studied in the past, pertaining to short fibres [10,11,12] and flake/platelet reinforcements [13,14]. Most of the theories for flakes are based on the knowledge from the behaviour of short fibres. Indeed in both the cases stress is transferred to the reinforcement through the interface between the matrix and the reinforcement. A brief overview of the key concepts involved is given the following subsections. For more detailed information on the formulation the reader is referred to the citations.

2.1 Strength of discontinuous composites

An elastic reinforcement in an elastic matrix is considered by Cox [10,15] with a perfectly bonded interface except for the end surfaces. Usually the matrix has a lower modulus than the reinforcement, hence the strain induced locally in the fibre is less than the matrix for carrying a particular far-field stress. Thus a shear stress is induced at the interface near the ends of the reinforcement and it drops to zero along the length of the fibre as shown in second quadrant of Figure 1. This non constant shear stress causes a non-linear buildup of normal stress in the reinforcement for maintaining an equilibrium state in the fibre (shown in third quadrant of Figure 1). In this theory the interactions between adjacent reinforcements and stress concentration issues due to the discontinuities are not considered.

Kelly [11] defines a similar phenomenon as Cox, but considers an elastic reinforcement in a plastic matrix. The matrix is assumed to flow plastically and maintain a constant shear stress at the interface (shown in the first quadrant of Figure 1). The transfer of shear into normal stress occurs in a so-called transfer length or the ineffective length from the free ends of the reinforcement. With increasing length of the reinforcement for the transfer of stresses, the buildup of stress in the reinforcement rises linearly till its ultimate load carrying capacity is reached. It is shown in the fourth quadrant of Figure 1. Any further increase in stress would rupture the short reinforcement. Hence if the length of the reinforcement is larger than a critical length (l_c) the reinforcement will be utilised to its full potential and will fail eventually. On the other hand for the reinforcements smaller than the critical length, the interfacial strength is the weak link and it fails before any stress in the reinforcement could reach the failure stress and consequently is pulled out due to debonding. Thus the critical length provides a transition between the two failure modes. Similar to Cox, interactions between reinforcements and stress concentrations are not taken into account.

Riley [12] and Piggot [14] consider interaction between the reinforcements. The former deals with short fibres and the latter with platelets following the fundamental principles of Kelly [11]. The load dropped by one fibre/flake near its end is shared by the surrounding flakes locally and hence stress concentrations arise along the length of the bridging reinforcements. Piggot [14] suggests that the effect of shape of the flakes either round or rectangle does show some effects in the stress distribution within the flake. On the other hand the effect of aspect ratio (length to thickness) was found to be influential in the case of circular flakes due to circular symmetry, but not in the case of rectangular flakes. Similarly the packing arrangement also influences the stress profile of the flakes. The load dropped at the end of a flake appears as a peak in the stress profile of the neighbouring flake locally at the discontinuity. If the packing arrangement is modified then the number of stress peaks and the distance between the peaks in the stress profile varies.

In all the cases the average tensile stress in the reinforcement is less than the matrix due to the tapered stress profile at the ends, implying that these materials can almost not reach the continuous reinforcement properties [16]. Considering a one dimensional approximation of the flake reinforcements, the length of the reinforcement should be around 50 times the critical length to reach

a stress level of 99% of the fibres' maximum load carrying capacity [17]

2.2 Modulus of discontinuous composites

Similar to the strength theories, the modulus has also been approximated for different types of discontinuous composites. Cox [10,15] uses the rule of mixtures to approximate the longitudinal modulus of aligned discontinuous composites. A correction factor is defined to account for the effect of fibre length and is based on the shear transfer principle discussed in section 2.1. The correction factor depends on the fibre volume fraction, shear modulus of matrix and the aspect ratio [16]. For the case of non-aligned discontinuous composites, Krenchel [18] defined an efficiency factor for the orientations. The factor tends to unity for an aligned fibre system with respect to the direction of stress and for other orientations it is a weighted summation of the orientation contribution, weighted with the proportion of fibres in a particular orientation. Padawer and Beecher [13] based on Cox [10] defined reduction factors for planar reinforcements to be used with the rule of mixtures, namely the modulus reduction factor (MRF) which is a function of flake volume fraction, aspect ratio and shear stiffness of the matrix.

2.3 Essentials for flake-reinforced composites and the underlying problem

From the analyses in the overviews above, analogous to the load transfer mechanism in a SFRC, the applied external load is transferred from the matrix to the flake by interfacial shear near the ends of the flakes. It is then transformed into a normal stress along its length [10,11]. The failure occurs in a sequence of steps either initiated by micro-cracks in the matrix or by fibre-matrix interface debonding. This eventually leads to overloading of fibres (within a flake) and rupturing of flakes which in-turn overloads adjacent flakes. The accumulation of such fractures progresses until the complete breakdown of the material. This underlying phenomenon is considered as the basis for the problem studied herein.

The studies carried out in the literature assume the flakes to be made of a homogenous material such as metal, glass or thin mica flakes. In the present investigation the flakes are chopped pieces of composite itself (recyclate), which could consist of woven fabric or a unidirectional material. However, in this study the flakes are made of woven fabric as stated in section 3.1.

Even though macroscopically F-RC is considered as quasi-isotropic, in the scale of the flakes, which is in between the macro and meso scale, it has a strong directional dependence arising due to the constitution of the flakes. The size and orientation of the flake with respect to the material axes and the directional properties of the flakes are the primary variables which influence the properties of F-RC such as stiffness and strength. Statistical distributions can be used to describe the randomness in the size due to the grinding process and the process induced orientations of flakes in the F-RC. Figure 2 shows a sample of ground flakes and Figure 3 shows an F-RC plate.

This article focuses on understanding and characterising the mechanical properties and identification of various failure phenomena in such compression moulded F-RC plates, produced from the scrap of woven glass fabric/thermoplastic polyurethane (TPU) 'parent composite'. In the following sections, details on the material used and the experimental investigations carried out are presented. The results of the experimental investigations are discussed. A suitable phenomenological model is devised based on the observations and measured distributions of the variables and is compared with the experiments and reference values from the parent material and similar discontinuous composite materials.

3 Materials and Experimental Methods

The recycled flakes (recyclate) and the compression moulded reinforced plate material used in this study were provided by CATO Composites Innovations B.V.

3.1 Materials

The parent laminate material comprises of TPU matrix reinforced with 2/2 twill weave glass fabric with a fibre volume fraction of 45%. The scrap material is ground into flakes as shown in Figure 2. Figure 2(a) and 2(b) show the flakes of material type A and B respectively. The material type A and B differ only by the number of layers of fabric reinforcement in the parent laminate. Type A has three layers and B comprises of two layers. During the grinding process the type A has been delaminated and hence some of the type A flakes do not have three layers. The ground flakes were then sieved with a mesh opening dimension of 10 - 15 mm in the case of material type A and 20 mm in the case of type B. The sieve sizes chosen for this study are independent of the material constitution and are

based on the nominal output size of the grinding process. A sieve size of 20 mm could not be used with type A material since the grinding process yielded sizes in the range less than 20 mm. Further the type B sieved flakes are segregated into several classes as shown in Table 1.

The mould cavity 200x200x2 mm^3 is filled with a determined quantity of a class of sieved flakes and is subjected to a compression moulding cycle. The moulding temperature was maintained at 220 degree Celsius and the pressure was set to 90 bars. The variation of the thickness in a plate was measured to be within ±0.3 mm.

The tensile specimens were cut from the moulded plates using a diamond saw to 25 mm in width and 200 mm in length. The width of the specimen was chosen to have a reduced size-effect with respect to the size of the flakes. The edges of the plates were removed before cutting. Five specimens were cut in three different orientations from the plate as shown in Figure 3. For the 45 degree specimens three plates from the same moulding batch were used to prepare five specimens. Different orientations of the specimens are chosen to quantify the effect of flow induced orientations of the flakes on the properties of the moulded plate.

3.2 Experimental Methods

The experimental study is centered on the uniaxial tensile test complemented with several other methods for a comprehensive characterisation of the F-RC plate at all the aforementioned scales. The test matrix is shown in the Table 1.

3.2.1 Flake size measurement, volume fraction measurement and Microscopic examination

The grinding process can be considered as a stochastic process in which the size variation is very much apparent. The sieving process helps to narrow down to a specific range of size after grinding. Even then every flake is different from each other. The size of the flakes are measured by image processing techniques using ImageJ [19] to determine the actual size range that can be expected in a moulded F-RC plate of a specified class.

Images of the sampled flakes from each class of size are photographed on a contrasting background. A ruler with reference markings and the flakes are laid flat so that the projected image corresponds to the area of the flake (Figure 2). The marking on the ruler is used to scale the image pixels to millimeters. Each image is converted to gray scale and is transformed to a binary mask by thresholding the gray scale values as shown in Figure 4. The segmented binary mask is then analysed for particles (flakes) greater than a certain area value to eliminate any false detection of the artifacts created during image segmentation. The area of the particle is constrained to fit an ellipse and the dimensions of the fitted ellipses are extracted.

Since the process scrap contains resin free regions near the outer edges of the parent laminates, after the grinding process the flakes might not have the same volume fractions as the parent laminate. Hence the volume fractions are measured on the final moulded F-RC specimens with its mass and volume according to ASTM D3171 [20]. The measurement is done after the tensile coupons are prepared.

A few regions of the plate were cut into small pieces revealing the cross section of the plate and were observed using optical microscopy.

3.2.2 Uniaxial tensile test

Uniaxial tensile tests are performed according to ISO527-4 [21] to determine the mechanical properties of F-RC plates. The applied strain rate for all the specimens are maintained constant at 1 mm/min and the specimens were loaded till failure. Hydraulic clamps were used to clamp the specimens in the machine (Zwick Z5.0) heads. The specimens were tested without end tabs and taper in the width direction, since a considerable amount of stress concentration regions are already present in the material. It is assumed that one of those regions might become a weak link and divert the crack initiation away from the clamps.

The strength data presented in this study corresponds to the ultimate stress reached in the tensile specimens, which is the ratio of maximum force borne by the specimen and the initial cross sectional area. The modulus is calculated by linearizing the stress-strain measurements between 0.05% to 0.25% strain according to ISO527-4. The strain in the specimen during the tensile testing was measured with a Laser Speckle Extensometer (LSE). The LSE is calibrated with a graticule (calibration ruler) before every batch of specimens are tested, to prevent any misalignment due to small movements of the camera support. The gauge length for the strain measurements were set at 50 mm. A digital single lens reflex camera was used to record the failure process.

3.2.3 SEM Fractography

The fracture surface is analysed with a scanning electron microscope (SEM) to examine the failure mechanism. The failure surface is sputter coated with a thin layer of gold for the conductivity. It prevents the local charging-up of the non-conductive specimen surface due to the electron beam and avoids causing artifacts in the SEM micrographs.

S.No.	Material Type	Sieve Size (mm)	No. of Specimens for Tensile Testing		
			Specimen Orientation (degrees)		
			0°	90°	45°
1	A	10-15	5	5	-
2	B	20:Fine	-	5	5
3	B	Middle	-	5	5
4	B	Coarse	-	5	5
5	B	Mixed1	-	10	-
6	B	Mixed2	-	5	5

S.No. 2-6 have the same sieve opening of 20 mm but segregated to different classes within the size.

Table 1. Test Matrix

4 Results

4.1 Flake size measurement

In the case of irregularly shaped flake reinforcements the definition of the size of a flake has considerable complexity. Since the flakes are irregular in shape, many size measures are possible [22]. In this study an equivalent size is determined by fitting an ellipse to the flake by constraining the area of the flake with image processing techniques (section 3.2.1). The major axis dimension for different classes of flakes is extracted from the software and is fitted with a lognormal distribution as shown in Figure 5. Only a limited number of flake samples were measurable for type B flakes amidst fine matrix dust and loose particles. From the density functions it can be seen that the mean value of size between different classes are not far apart. The mode of the distribution represented by the peak value of the density curve gives the most probable size occurring in the sampled flakes. For type B flakes the modes are very close to each other. The spread in the flake size within a class of type B is large when compared to the type A which is apparent from the width of density function. A narrow density function signifies a narrow range of flake size variation.

4.2 Volume fraction approximation and micrographs

The fibre volume fraction of each tensile specimen was approximated by its mass and volume and was found to be close to each other. The Figure 6 shows the values for each set of specimens with their standard deviations.

4.2.1 Cross sectional micrography

The micrographs of the cross sections obtained from the polished samples were examined for voids and other pre-existing defects in an as-moulded state. Figure 7 shows one of the micrographs. Debonded fibre matrix interface and matrix micro-cracks emanating from these debonded regions were observed. The debonded regions or the micro-cracks can become a crack initiator upon loading. There were only very few void regions observed. Resin pockets between the flakes were observed more frequently, which are a potential weak link during loading.

The cross sectional image of the plate usually reveals the orientation of the fibres from the ellipticity in the cross section of oriented fibres, created by the cutting plane. In this case, each flake is made up of a piece of woven fabric, which in turn is made up of bundles of fibre filaments. Finding which bundle corresponds to which flake is not trivial. A robust methodology based on the analysis of successive image slices of the same sample has to be developed and is not in the scope of this study.

4.3 Uniaxial Tensile test

Specimens corresponding to three different orientations from the plate as shown in Table 1 and Figure 3 were tested in order to investigate orientation effects and the randomness in the flake distribution. The results in the plot show no significant difference in the modulus or the strength between different orientations of specimens. All the values are within the measurement deviations. It can be inferred that the F-RC plates appear to show an in-plane isotropic behaviour in a macroscopic scale. In other words: the flakes are randomly oriented.

The typical stress-strain curve for two types of distinct behaviours observed is shown in Figure 8. A linear build-up of stresses can be observed in both cases until a certain point at which the behaviour tends to become non-linear. The peculiarity arises in the strain to failure. One of the specimens from the same plate fails with a much lower strain than the other for a similar strength value. Upon observing

the failure type of the specimens as shown in Figure 9, it was apparent that the specimen with large energy absorption has a larger failure surface with considerable shearing. One of the flakes in the failure surface was delaminated absorbing the considerable energy spent during failure as seen in the first one third of the Figure 9(b).

In most of the cases the strain localises in many spots at approximately same moments in time. Upon further loading the weakest of them initiates a crack and then the damage evolves as the crack progresses through the material in the width direction leading to catastrophic failure. These localisation phenomena are assumed to be one of the causes for the non-linear behaviour apart from the complex interactions between the planar flakes. The presence of a poor interface becomes a site for crack initiation.

Figure 9(a) shows the failure region in which it can be seen that the cracks avoid the flakes and change direction via a least resistance path around the flake. As seen in the critical length calculation in section 5.2 and Table 3, almost all the flakes are below the calculated critical length when compared to Figure 5, assuming a one-dimensional approximation. Hence the flakes might not be fully loaded and failure by pull-out with insufficient shear strength of the interface occurs. In other words: matrix failure is dominant in the observed cases.

Due to the presence of loose fibres in the system, the observed effects are not completely conclusive since there are more effects viz. crack bridging, two dimensional complex interactions between the flakes and embrittlement of the matrix due to the loose particles between the flakes.

The plots in Figures 10 and 11 show the strength and modulus. The values are normalised with respect to the parent material for comparison. The typical value of E-Modulus for the parent is 19 GPa and the strength is around 325 MPa. It can be seen that there is no significant difference in the values of modulus and strength between the size classes of type B and between type A and B as well. This might be due to the similar size ranges of the flakes for all the classes as seen in Figure 5.

4.4 Failure surface analysis

SEM micrographs of the fracture surface are shown in Figure 12. In Figure 12(a) good adhesion of the matrix to the fibre can be observed as there exist remains of matrix on the fibre even after failure representing a cohesive failure and yield lips can also be seen. In Figure 12(b) the adhesion appears to be poor since the flakes have been separated and a clean fibre surface is visible.

5 Phenomenological semi-analytical model

Based on the theoretical literature survey, approximations for the longitudinal elastic modulus and tensile strength have been calculated. In this section they will be compared with the experimental results.

5.1 Modulus Approximation

Based on Padawers' [13] approach discussed in section 2.2, a rule of mixtures with a modulus reduction factor (MRF) is considered for approximating the modulus of the flake-reinforced composite. The following equations give the elastic modulus for a discontinuous planar reinforced material assuming the matrix and reinforcements are linearly elastic, flakes are of uniform size and thickness, regular pattern of alignment and a perfect flake-matrix adhesion.

$$E_C = E_f \, v_f \, MRF + E_m\left(1 - v_f\right)$$

$$MRF = \left(1 - \frac{\tanh(u)}{u}\right)$$

Where,

$$u = \alpha \left[\frac{G_m v_f}{E_f(1 - v_f)}\right]^{1/2}$$

$$\alpha = \bar{l}/t$$

The variables with subscript f are related to the reinforcement phase and with subscript m are related to the matrix phase. v_x refers to the volume fraction of the phase. E_x to the elasticity modulus and G_x to the shear modulus where $x \in \{f, m\}$. $\bar{l}$ is the mean length of the flake and t represents the thickness.

Parameter	Value
G_m	8 MPa
E_m	150 MPa
E_f	19000 MPa
$\bar{l}$	16 mm
d_f	10 μm

The values of the matrix correspond to Desmopan 385.

Table 2. Flake-matrix system properties.

The value of the modulus of the flake phase corresponds to the modulus of the parent of the

recyclate. By substituting the values for the current system as shown in the Tables 2 and 3, the modulus is severely underestimated due to a very low aspect ratio. The flakes are not homogeneous and are in the form of bundles of fibres and also presence of loose fibres in the moulded plates is observed. Hence, it is relevant to use the fibre diameter d_f to calculate the aspect ratio. Since the pattern of the reinforcement (weave pattern) is preserved in the flakes, the modulus of the combined fibre-matrix system can be assumed approximately equal to the parent laminate (locally within a flake) as given in the Table 2.

Upon calculation, the modulus value resulted in around 5168 MPa for an aspect ratio ($\bar{l}/d_f$) of 1600. It corresponds quite close to the experimental value obtained. It is worth to note that the actual situation inside the specimen is violated greatly from the assumptions in the model. Further investigation is required to refine the model according to the system under study. A more detailed comparison of values is given in section 6.

5.2 Strength Approximation

Strength prediction is not straightforward and is greatly influenced by the inhomogeneities in the material, stress concentrations [13] fibre/fibre interactions [12], stacking pattern and shape of flakes [14]. These give rise to the actual mechanism of failure. The failure is primarily due to interface failure, resin pocket/matrix failure or flake rupture. The knowledge of the failure mechanism plays a critical role in the strength prediction.

The Kelly-Tyson [11] model of load transfer in discontinuous systems is widely accepted and is used for predicting the strength in this section. The major assumptions involved are perfectly bonded interface, perfectly plastic matrix and no stress transfer takes place in the end faces of the reinforcements.

The average longitudinal stress of a discontinuous system can be approximated by the rule of mixtures as follows:

$$\sigma_C = \bar{\sigma}_f \, v_f + \sigma'_m(1 - v_f) \ldots \qquad \text{Eq. 1}$$

Where the subscript notations are similar to the ones used in section 5.1 for the modulus approximation. Here $\bar{\sigma}_f$ denotes an average stress in the flakes, given by the area under the curve show in the lower quadrants of Figure 1 and σ'_m denotes the matrix stress at failure.

Since the reinforcements have different lengths and orientations, the average stress in the reinforcement can be modified by correction factors χ_L, χ_O where the subscripts refer to the length and orientation. Based on Kelly's model, χ_L is a function of the critical length and the flake length distribution and χ_O is a function of the orientation distribution [23]. The average stress $\bar{\sigma}_f$ in Eq. 1 can be replaced by the product $\chi_L \chi_O \bar{\sigma}$. The values for the factors are as below:

$$\chi_L = \chi_L(l) = \begin{cases} \dfrac{1}{2l_C}; l < l_c & (a) \\ \left(1 - \dfrac{l_c}{2l}\right); \; l > l_c & (b) \end{cases} \qquad \ldots \text{Eq. 2}$$

where, $l_c = \dfrac{\sigma_f^u t}{2\tau_i}$

and $\chi_O = \frac{1}{\pi}$ …Eq. 3

The component of stress borne by the flakes larger than the critical length is given by Eq.2 (a) and less than the critical length is given by Eq.2 (b). Since there exists a distribution of length of the flakes, the contributions can be summed over the entire domain of l. l_c is the critical length and is dependent on the material-combination. The superscript u specifies that it is the ultimate property value. t denotes the thickness of the flake and τ_i denotes the interfacial shear strength of the interface. Using the Von Mises criterion, the shear strength of the matrix is approximated at the yield stress of the matrix, with $\sigma_m^{yield}/\sqrt{3}$, a typical value is given in Table 3.

Assuming uniformly distributed flakes based on the experimentally observed in-plane isotropic behaviour, the orientation efficiency factor χ_O can be assigned a value of $1/\pi$, having equal probability over the range of π radians.

In section 4.1 it was observed that the length of the flakes is not constant but is distributed over a range of values. Consider $p(l)$ being a lognormally distributed probability density function of the length of the flakes such that:

$$p(l) = \frac{1}{s\sqrt{2\pi}\, l} e^{\frac{-(\ln(l)-m)^2}{2s^2}} \qquad \ldots \text{Eq. 4}$$

and

$$\int_0^\infty p(l) dl = 1$$

where s is the standard deviation and m is the mean value. The lognormal distribution can be perceived as the values of l are normally distributed in the log space.

Upon using the distribution of flake lengths Eq.4. in Eq. 2. The overall χ_L can be obtained as:

$$\chi_L = \int_{l_{lb}}^{l_c} \left(\frac{l}{l_{mean}}\right)\left(\frac{l}{2l_c}\right) p(l)dl + \int_{l_c}^{l_{ub}} \left(\frac{l}{l_{mean}}\right)\left(1 - \frac{l_c}{2l}\right) p(l)dl \quad \text{…Eq. 5}$$

Where,

$$l_{mean} = \int_0^{\infty} l\, p(l)dl = \int_{l_{lb}}^{l_{ub}} l\, p(l)dl$$

It can be noted from Eq. 5 that the integrations are done over the ranges specified in Eq.2 (a) and (b) between the measured lower bound length l_{lb} and upper bound length l_{ub} of the flakes. The averaging process in Eq. 5 is shown in figure 14 pictorially. The typical values used for the calculations are shown in Table 3.

Parameter	Value	Units
σ_f^u	325	MPa
t	0.6†	mm
$\tau_i = \sigma_m^{yield}/\sqrt{3}$	7.5/√3 *	MPa
σ_m'	A:41 B:39**	MPa
$v_f\ (type\ A)$	0.325†	-
$v_f\ (type\ B)$	0.28†	-
l_c	22.51	mm

* Typical value for TPU

** Experimentally observed value at the fracture strain

† **Measured values**

Table 3. Typical values used in the calculations.

6 Discussion

The typical values of the experimentally determined average strength and stiffness are shown in Table 4. Since negligible difference was observed between different orientations and class sizes. The values are averaged over the entire specimen set. The table also shows the calculated values from the analytical model discussed in section 5. The values are quite representative in-spite of the presence of loose particles in the system. The deviation in the values is caused due to multitude of possibilities such as complex stress interactions and mixed failure modes. Presence of loose fibres could bridge a crack and could provide local strengthening. Taking into account such phenomena including the orientation effects of the flakes, a more appropriate model can be developed further in future.

Material	Density (g/cm^3)	E Modulus (GPa)	Strength (MPa)
Type A	1.59	5.82	41.24
Type B	1.64	5.48	39.58
Calculated	-	5.16	A : 34.57 B : 39.20

Table 4 Typical properties measured and calculated for F-RC plate specimens

Some reference values for non-woven glass-mat, short and long fibre composites were obtained from [24]. It gives a comparative position of F-RC amidst other discontinuous reinforced composites. The matrix chosen for comparison was based on closeness to the TPU in mechanical properties among the others. A similar volume fraction of fibres of around 30% was chosen for comparison. On comparison the glass-mat with a polypropylene (PP) matrix has modulus around 5 GPa and strength around 75 MPa for a material density of 1.13 g/cm^3. On the other hand, a SFRC with a PP matrix has a modulus of 6 GPa and strength of 55 MPa for a material density of 1.15 g/cm^3. It can be seen from comparison that the E-modulus is close to the reference values and the strength increases significantly with reinforcement length.

By properly tuning the geometrical properties of the flakes, overlap between the flakes and interface properties, and by reducing the voids and resin pockets, a potential of achieving much better mechanical properties is expected.

7 Conclusions

An experimental investigation was carried out to characterise the mechanical behaviour of flake reinforced thermoplastic composite plates under uniaxial tension. Instead of granulating or chopping composite scrap into a short fibre compound, the scrap was ground in the form of flakes to potentially provide a two dimensional reinforcement in the flake-scale. The size of the flakes was varied between plate samples to investigate its effect. The

relative distance between the mean size of the flakes corresponding to different size classes was found to be not far apart. Moreover, there was a considerable spread in the size distribution of the flakes within each class. Consequently the mechanical properties were found to be in the same order between different plate samples with varying flake sizes and less when compared to the parent. The experimental results also show that the randomness in the flakes' orientation gives rise to an in-plane isotropic behaviour. The analytical model incorporating the measured flake size distribution provided considerably close results for the stiffness and in the case of strength, other effects such as overlap, crack bridging, orientation of flakes have to be included in the model for a more conclusive result. Further investigations on the fibre matrix adhesion with respect to the processing conditions are necessary for a critical evaluation of the failure initiation. A parametric analysis of the effects of flakes has to be carried out in future for a more critical evaluation of the influential parameters. In a practical perspective, by analyzing the behaviour of the flakes in the F-RC, the processing of recycled composites can be further improved.

Acknowledgements

The authors are thankful to the project leader CATO Composites Innovations B.V., Doesburg (NL) for providing the recycled compression moulded composite materials. The funding provided by the funding partner DPI Value Center, Eindhoven (NL) is gratefully acknowledged.

References

[1] Richard Stewart, Thermoplastic composites - recyclable and fast to process, *Reinforced Plastics*, Volume 55, Issue 3, May–June 2011, Pages 22-28, from http://www.sciencedirect.com/science/article/pii/S003436171170073X

[2] HexMC® Guide, Hexcel Corp., Oct. 2008. Web. 01 May'13.,http://www.hexcel.com/Resources/UserGuides/HexMC_UserGuide.pdf

[3] Jack D. Fudge, PE., "Chopped prepregs - a compelling performance and cost alternative material form", *41st International SAMPE Technical Conference, Kansas, October 19-22*, 2009.

[4] "Boeing 787 Features Composite Window Frames." *Reinforced Plastics*, 51:3, pg 4, 2007. ScienceDirect. Web. 27 May 2013.

[5] Black, Sara. "Redesigning for Simplicity and Economy." *High-Performance Composites*. Composites World, 2 Jan. 2012. Web. 01 June 2013., http://www.compositesworld.com/articles/redesigning-for-simplicity-and-economy.

[6] N.E. Dowling. "*Mechanical behavior of materials"*. 2nd edition, Prentice Hall, 2007.

[7] C.R. Chiang. "A statistical theory of the tensile strength of short fiber reinforced composites". *Composite Science and Technology*, 50, pp 479-482, 1994.

[8] R.J. Kuriger, M. Khairul Alam and Davi P. Anderson "Strength prediction of partially aligned discontinuous fiber reinforced composites". *Journal of Materials Research*, No. 16, pp 226-232, 2001.

[9] Thanh Trung Do and Dong Joo Lee. "Degradation in tensile properties with overlapped and discontinuous fabric preforms". *Advanced Composite Materials*, 20:5, pp 443-462, 2011.

[10] Cox H.L. "The elasticity and strength of paper and other fibrous materials". *British Journal of Applied Physics*., 3, pp 72-79, 1952.

[11] Kelly A, Tyson WR. "Tensile properties of fibre-reinforced metals: copper/tungsten and copper/molybdenum". Journal of Mechanics and Physics of Solids, 13, pp 329-350, 1965.

[12] V.R. Riley. "Fibre/Fibre interaction". *Journal of Composite Materials*, 2, p 436, 1968.

[13] G.E Padawer et al., "On the strength and stiffness of planar reinforced plastic resins". *Polymer Engineering & Science*, 1970.

[14] B. Glavinchevski, M. Piggott. "Steel disc reinforced polycarbonate", *Journal of Materials Science*, 8, pp 1373-1382, 1973.

[15] Folkes, M. J. "*Short Fibre Reinforced Thermoplastics*". Research Studies Press, 1982.

[16] Clegg, D. W. and Collyer, A. A. "*Mechanical Properties of Reinforced Thermoplastics*". Elsevier Applied Science Publishers, 1986.

[17] B.D. Agarwal, L.J. Broutman. "*Analysis and performance of fiber composites*". 2nd edition, John Wiley, 1990.

[18] Krenchel, H. "*Fibre Reinforcement*". Akademisk forlag, Copenhagen. 1964.

[19] Rasband, W.S. ImageJ, U. S. National Institutes of Health, Bethesda, Maryland, USA, http://imagej.nih.gov/ij/, 1997-2012.

[20] ASTM D3171 – 06, Standard Test Methods for Constituent Content of Composite Materials, 2006.

[21] ISO 527-4:1997, Plastics -- Determination of tensile properties -- Part 4: Test conditions for isotropic and orthotropic fibre-reinforced plastic composites, 1997.

[22] Merkus, HenkG., "*Particle size measurements*", pp 13-42, Springer Netherlands, 2009.

[23] Shao-Yun Fu, Bernd Lauke,. "Effects of Fiber Length and fiber orientation distribution on the tensile strength of short-fiber reinforced polymers", *Composite Science and Technology*, 56, pp 1179-1190, 1996.

[24] Biron, Michel. "*Thermoplastics and Thermoplastic Composites: Technical Information for Plastics Users*". Second edition, Elsevier, 2007.

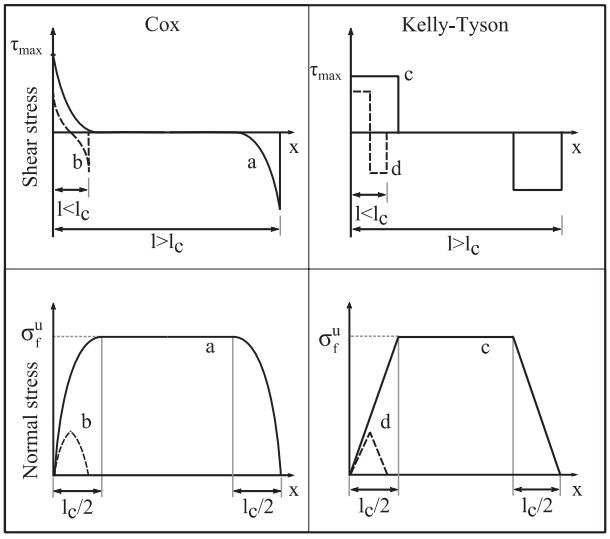

Load transfer mechanism

Fig. 1. Load transfer mechanism in a short fibre of length 'l' along its length (x-axis). The dotted lines show another case where fibre is shorter than critical length and subjected to a smaller load.

Fig. 2(a). Glass/TPU Type A flakes.

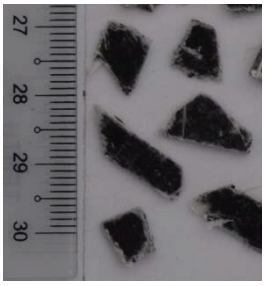

Fig. 2(b). Glass/TPU Type B flakes.

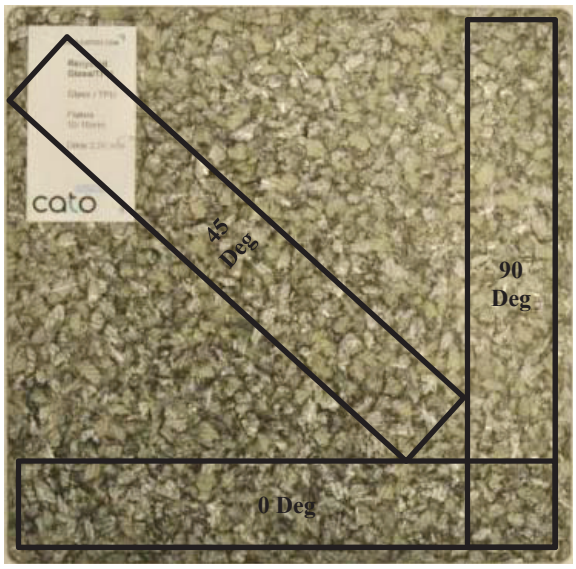

Fig. 3. Glass/TPU Type A plate showing the specimen orientations.

Fig. 4. Thresholded image of flakes.

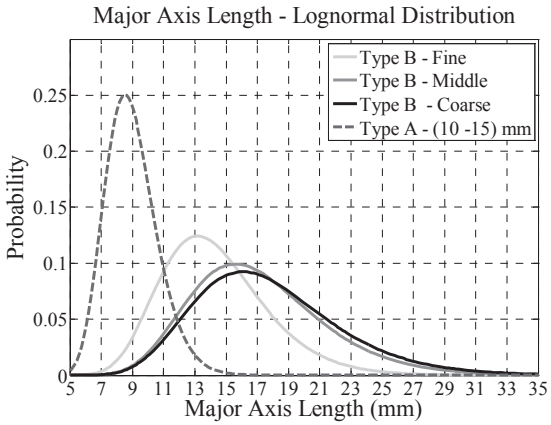

Fig. 5. Lognormal distribution of flake size/length.

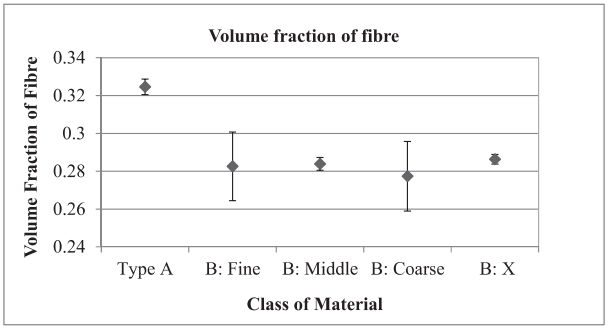

Fig. 6. Volume fraction of fibres of type A and type B tensile specimens, X denotes mixed class.

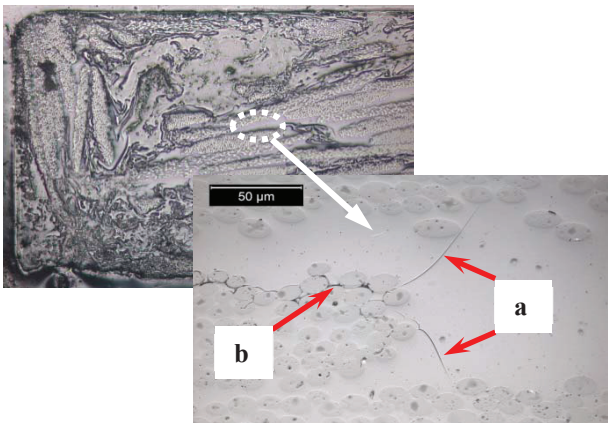

Fig. 7. Micrographs of the F-RC showing (before testing) a: matrix micro-cracks, b: fibre-matrix interface debonding.

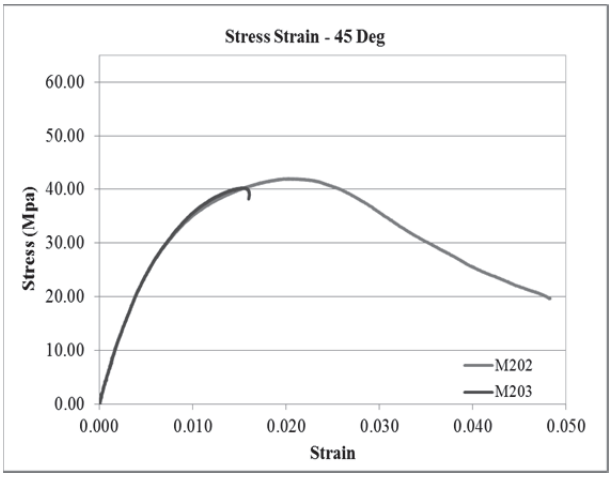

Fig. 8. Stress strain plot showing distinct behaviour.

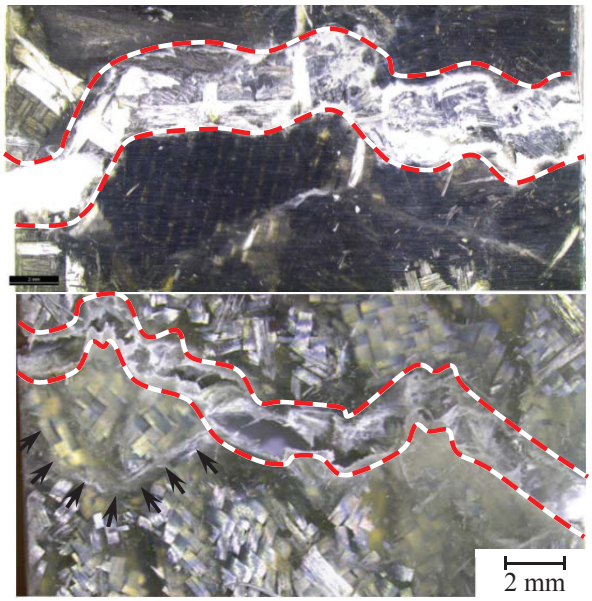

Fig. 9. Fracture in tensile two different specimens (bottom 9(a), top 9(b)), arrows point the strain localisation, dotted lines envelope the fracture path.

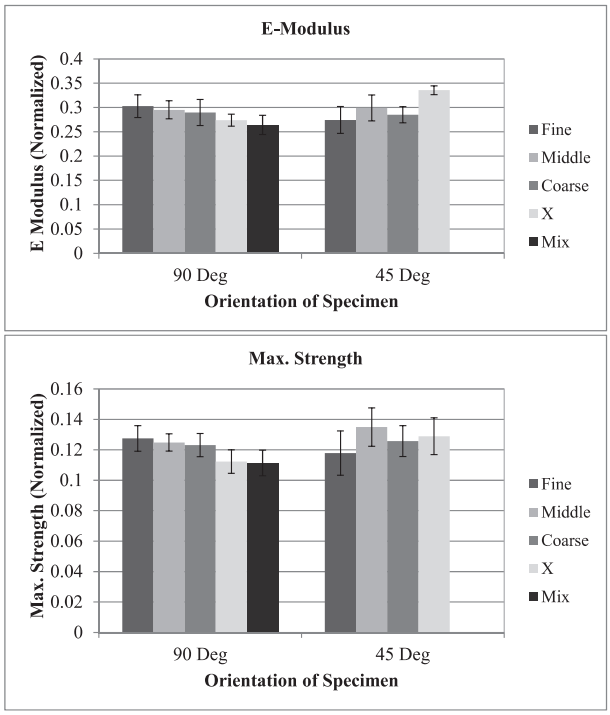

Fig. 10. (a), (b) E-Modulus and maximum strength of Type A F-RC specimens.

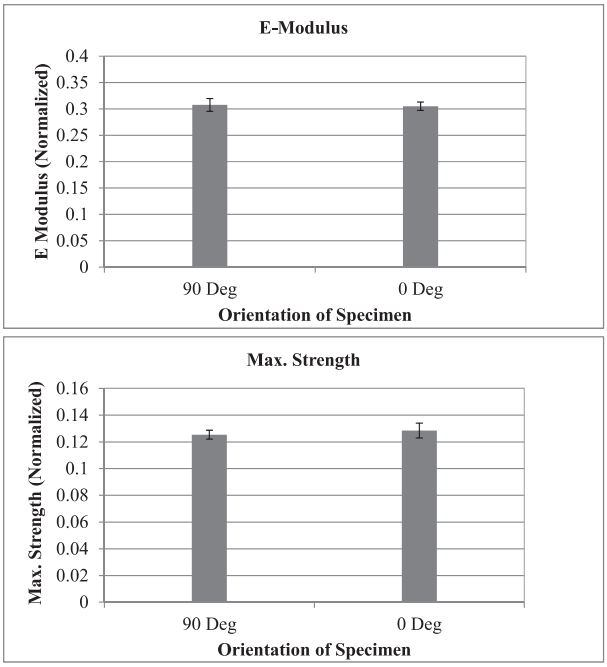

Fig. 11. (a), (b) E-Modulus and maximum strength of Type B F-RC specimens.

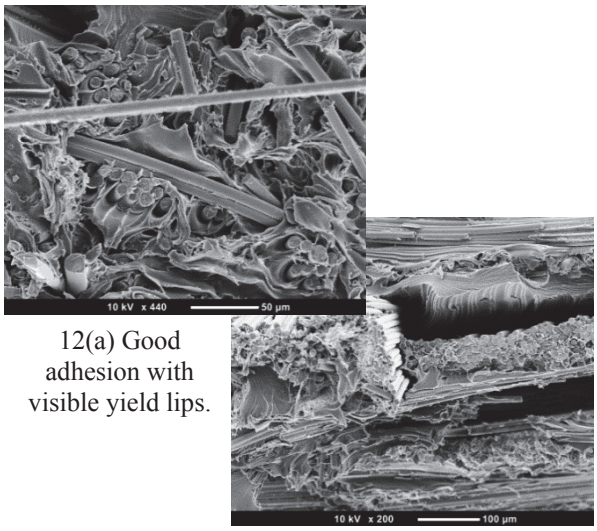

12(a) Good adhesion with visible yield lips.

12(b) Poor adhesion, and interface failure.

Fig. 12. SEM images of fracture surfaces.

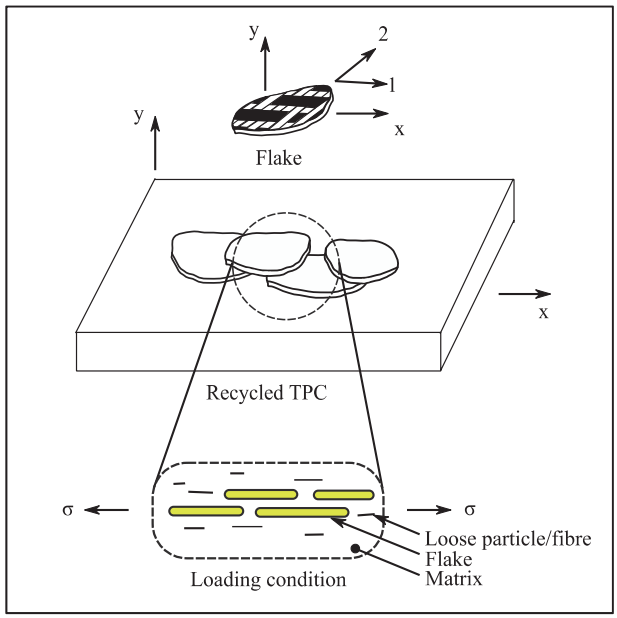

Fig. 13. Flake-matrix system. (top) flake with principle directions; (middle) sample F-RC place; (bottom) detailed view showing the cross sections of the flakes (fibre bundles within the flakes are not shown for brevity) and the presence of loose fibres (non-ideal system) in the matrix. A tensile load case is also shown.

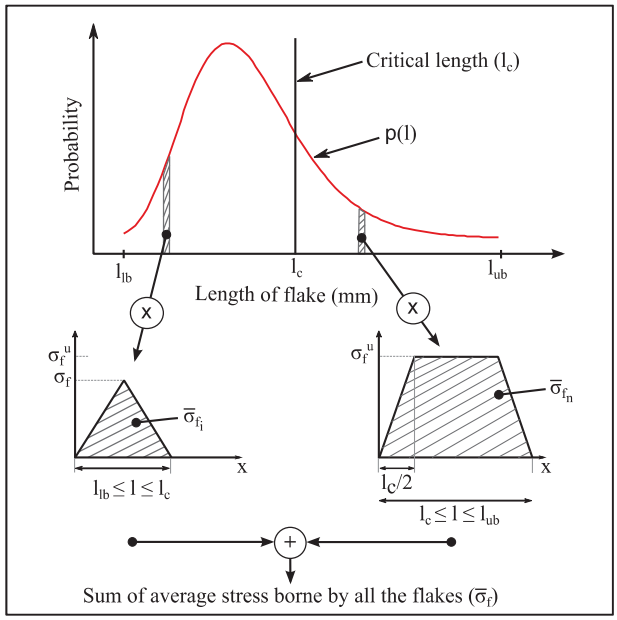

Fig. 14. Average stress borne by flakes of different length. (Section 5.2)